Available online at www.sciencedirect.com

ScienceDirect

Procedia IUTAM 26 (2018) 81–91

Procedia IUTAM

www.elsevier.com/locate/procedia

IUTAM Symposium Wind Waves, 4–8 September 2017, London, UK

Estimation of directional spectra from wave buoys for model validation

Richard M. Gorman

National Institute of Water and Atmospheric Research, Hamilton, 3216, New Zealand

Abstract

In this paper, we consider the problem of estimating a directional wave spectrum from 3-dimensional displacement data recorded by a wave buoy. We look at some of the limitations of existing methods to extend the "first five" directional moments directly obtainable from such data. With a view to providing the most detailed possible comparisons with directional spectra obtained from numerical models, we propose the use of a "diagnostic" directional spectrum, defined to be the closest possible spectrum to a given model spectrum that satisfies all measured directional moments. This method allows us to quantify the *minimum* error in a modelled directional spectrum consistent with a buoy record.

The new method is tested on a range of artificial test cases, and applied to data obtained from a wave buoy deployment off the New Zealand coast, in conjunction with outputs from a numerical spectral wave model simulation. It is shown that the method can provide satisfactory results in a wide range of conditions. Unlike existing approaches, the proposed method can accommodate sea states with more than two directional peaks, and can assist in removing spurious spectral energy arising from existing methods for estimating directional spectra from buoy data.

Peer-review under responsibility of the scientific committee of the IUTAM Symposium Wind Waves.

Keywords: wave buoy; directional wave spectrum; forecast verification

Email address: Richard.Gorman@niwa.co.nz

1. Introduction

Wave conditions in the ocean can be most thoroughly characterised by combining numerical modelling with measurements. *In situ* measurements from wave buoys are most commonly applied to model evaluation through comparison of derived wave statistics (e.g. significant wave height, mean wave direction, peak wave period). But a more thorough comparison of measurements with full directional spectra predicted by modern wave models could

2210-9838
Peer-review under responsibility of the scientific committee of the IUTAM Symposium Wind Waves.
10.1016/j.piutam.2018.03.008

offer greater diagnostic insight, allowing us, for example, to separately compare each component of a complex sea state.

Directional wave buoys work by making simultaneous measurements of a small number of signals, e.g. displacements in each of the 3 spatial dimensions. Fourier co- and cross-spectra between pairs of these signals can then be used to provide a limited estimate of the directional spectrum. That is, only the "first five" parameters moments of the directional distribution are obtained, which is insufficient for a full comparison with model spectra that typically have tens of directional degrees of freedom.

In the following section of this paper we review some existing approaches to the problem of extending beyond the measured "first five" moments to estimate a more complete directional wave spectrum from data. We then, in Section 3, propose a new method, which defines a "diagnostic" directional spectrum $S^{(d)}(f,\theta)$ for comparison with a given model directional spectrum $S^{(m)}(f,\theta)$, such that $S^{(d)}$ is the closest possible spectrum to $S^{(m)}$ that satisfies all measured directional moments. This method allows us to quantify the *minimum* error in a modelled directional spectrum consistent with a buoy record. The method is then applied firstly to some artificial test cases, then to directional data obtained from a wave buoy, in conjunction with outputs from a spectral wave forecast. A brief discussion of these results is then given in Section 4.

2. Fourier representation of sea state

Wave motions can be measured by a floating buoy, such as a Waverider™, that records accelerations in up to three dimensions, from which displacements can be computed by double integration of the signal.

First we consider a non-directional instrument that records only vertical motions. The vertical displacement Δz of the sea surface at a fixed position and time t can be represented as a sum of sinusoidal signals:

$$\Delta z(t) = \sum_{m=1}^{M} A_m \cos[-2\pi f_m t + \phi_m] \tag{1}$$

Here A_m is the amplitude, f_m the frequency, and φ_m the phase, of the m^{th} individual component.

Assuming random phases and summing the square of all amplitudes in a small range df of frequencies gives the wave frequency spectrum $S(f)$ of the wave signal:

$$\frac{1}{df}\sum_{f}^{f+df} \tfrac{1}{2}A_m^2 = S(f) \tag{2}$$

This can be computed as

$$S(f) = Z^* Z = |Z|^2 \tag{3}$$

from the Fourier transform

$$Z(f) = \int \Delta z(t) e^{-i2\pi f t} \mathrm{dt} \tag{4}$$

of the displacement signal.

Directional buoys can also measure horizontal displacements. Using the same sum of sinusoidal signals, these would be given as

$$\Delta x(t) = \sum_{m=1}^{M} A_m \cos\theta_m \sin[-2\pi f_m t + \phi_m] \tag{5}$$

and

$$\Delta y(t) = \sum_{m=1}^{M} A_m \sin\theta_m \sin[-2\pi f_m t + \phi_m] \tag{6}$$

which now include the propagation direction θ_m of each wave component.

Now we can sum the squares of all components within small ranges of both frequency and direction to obtain a directional spectrum

$$\frac{1}{df}\sum_{f}^{f+df}\frac{1}{d\theta}\sum_{\theta}^{\theta+d\theta}\frac{1}{2}A_m^2 = S(f,\theta) \tag{7}$$

We can attempt to estimate the directional spectrum using the Fourier transforms

$$X(f) = \int \Delta x(t) e^{-i2\pi f t}\mathrm{d}t \tag{8}$$

$$Y(f) = \int \Delta y(t) e^{-i2\pi f t}\mathrm{d}t \tag{9}$$

of the horizontal displacement as well as $Z(f)$ defined above, but this is restricted to the six possible co- and cross-spectra, which define specific directional moments of $S(f,\theta)$, i.e. (in the deep water case):

$$G_{zz} = Z^*Z = C_{zz} = \int_0^{2\pi} S(f,\theta)\, d\theta = S(f) \tag{10}$$

$$G_{zx} = Z^*Y = iQ_{zx} = i\int_0^{2\pi} S(f,\theta)\cos\theta\, d\theta \tag{11}$$

$$G_{zy} = Z^*Y = iQ_{zy} = i\int_0^{2\pi} S(f,\theta)\sin\theta\, d\theta \tag{12}$$

$$G_{xx} = X^*X = C_{xx} = \int_0^{2\pi} S(f,\theta)\cos^2\theta d\theta \tag{13}$$

$$G_{yy} = Y^*Y = C_{yy} = \int_0^{2\pi} S(f,\theta)\sin^2\theta\, d\theta \tag{14}$$

$$G_{xy} = X^*Y = C_{xy} = \int_0^{2\pi} S(f,\theta)\cos\theta\sin\theta\, d\theta \tag{15}$$

We note that only five of these terms are independent, with $C_{xx} + C_{yy} = C_{zz}$.

Another way of looking at the limited directional information available is to consider the normalised directional distribution $D(f,\theta)$, defined by

$$S(f,\theta) \tag{16}$$

Any function of direction can be represented as a Fourier sum

$$D(f,\theta) = \frac{1}{2\pi}+\frac{1}{\pi}\sum_{n=1}^{\infty}[a_n(f)\cos n\theta + b_n(f)\sin n\theta] \tag{17}$$

Of these terms, the co- and cross-spectra above that are obtainable from three-component buoy data can provide only $S(f)$, $a_1(f)$, $b_1(f)$, $a_2(f)$ and $b_2(f)$ (the so-called "first five" moments) using relationships described by Longuet-

Higgins et al [1]:

$$a_1 = \frac{-Q_{zy}}{\sqrt{(C_{xx} + C_{yy})C_{zz}}} \tag{18}$$

$$b_1 = \frac{-Q_{zx}}{\sqrt{(C_{xx} + C_{yy})C_{zz}}} \tag{19}$$

$$a_2 = \frac{(C_{yy} - C_{xx})}{(C_{xx} + C_{yy})} \tag{20}$$

$$b_2 = \frac{-2C_{xy}}{(C_{xx} + C_{yy})} \tag{21}$$

No measure of the higher terms is, however, available. This means that any attempt to represent the full directional distribution from buoy data must, in effect, introduce some additional criteria to supply estimates of the value of the higher components.

2.1 Approaches to the "first five" problem

The simplest approach to this problem is to assume that all the higher terms are zero [1]. By only including the most slowly varying terms, this approach can only represent broad directional distributions, with one or two peaks. We can illustrate this by some test cases in which we assume a "true" directional distribution with multiple peaks built by a weighted sum of simple parametric forms [1, 2]:

$$D(\theta) = \sum_{m=1}^{M} w_m \left[cos(\theta - \theta_{0,m})/2\right]^{p_m} \tag{22}$$

In which the mth component, with mean direction $\theta_{0,m}$ and directional spreading parameter p_m, contributes to the sum with weight w_m. Then we compute the directional moments and the first five parameters using Equations 10-15 and 18-21 above, to give the estimated directional distribution that the "first five" approximation would give.

Figure 1 shows an example with a single peak with a directional spread of 30° (p = 30), typical of moderately-developed swell. We see that the "first five" approximation ("LH unweighted") overestimates the spread of this peak. It also produces an artificial peak at 180° from the true peak, and unphysical negative values in between.

Longuet-Higgins et al [1] addressed the problem of negative spectral densities by applying weights to the terms in the sum (Eqn 17). While this makes negative values impossible, it does not improve the ability to represent narrow spectra. Indeed, in the example shown in Figure 1, this method ("weighted LH") produces an even broader peak.

A second example (Figure 2) shows a case with three peaks in the input directional distribution, centred on 60°, 150° and 220°, with directional spreads of 15°, 30° and 10°, respectively. The unweighted "first five" approximation results in overly broad representations of two of these peaks, but the third being missed, while the weighted version shows very little ability to resolve any of the peaks.

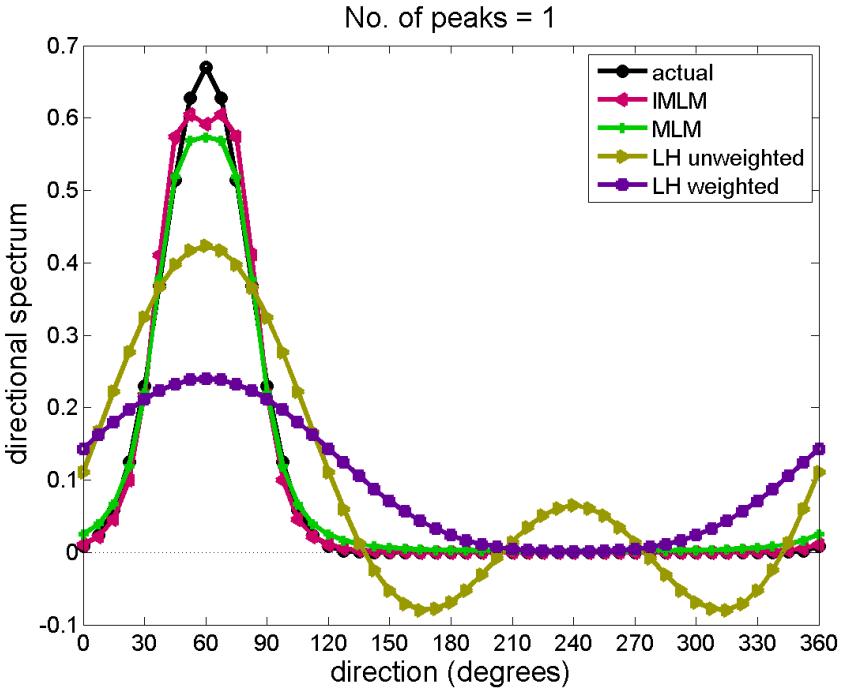

Figure 1 Comparison of a directional distribution of the form $D(\theta) = [\cos(\theta - \theta_0)/2]^p$, with peak direction $\theta_0 = 60°$ and spreading parameter $p = 30$ (black) with the distributions obtained by fitting these data by four methods: MLM [3, 4], IMLM [5], and the unweighted and weighted methods of Longuet-Higgins et al [1].

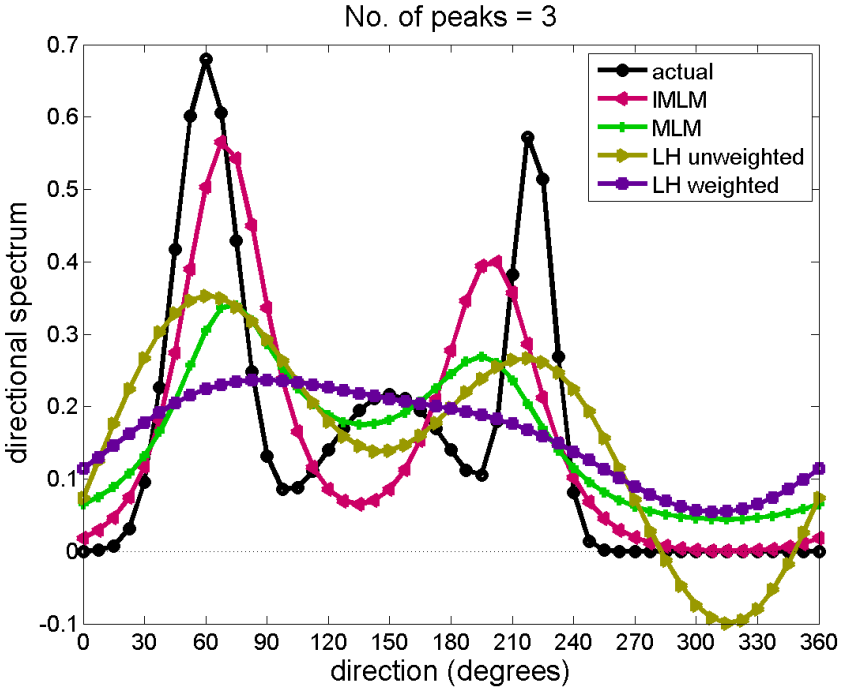

Figure 2 Comparison of a directional distribution combining a weighted sum of three distributions of the form $D(\theta) = [\cos(\theta - \theta_0)/2]^p$ (black) with the distributions obtained by fitting these data by four methods: MLM [3, 4], IMLM [5], and the unweighted and weighted methods of Longuet-Higgins et al [1].

For unimodal spectra, it is possible to provide a better representation by fitting a parametric form, as done by Mitsuyasu et al [2] with the form we used in Eqn (22) above. But clearly this is not suitable for mixed sea states.

Other approaches are based on some metric of statistical "quality" to determine a best fit. Such methods include the Maximum Likelihood Method (MLM) in original and extended versions [3, 4], the Iterated Maximum Likelihood Method (IMLM) [5], the Maximum Entropy Method (MEM) [6], and the Bayesian Method (BM) [7]. We do not present the details of all of those methods here, but note that many of these methods have been incorporated in software and tested, e.g. the DIWASP Matlab package [8], and described in reviews, e.g. by Benoit et al [9].

It is noted that some of these methods can be applied more generally, i.e. to data from other combinations of sensors (e.g. arrays of multiple wire sensors, pitch-roll buoys), supplying more than the three signals available from a Directional Waverider. In such cases, the number of terms fitted in Eqn 17 can be extended beyond the first five. While other methods may be more suited to other data sources, it is observed that the Iterated Maximum Likelihood Method is generally a good choice for directional wave buoy data, which is our main focus. Hence we will concentrate on the IMLM as a benchmark for currently-available methods, and not include any results from the MEM or BD methods in this paper. In particular, the IMLM is capable of reproducing narrower directional spreads than the unweighted and weighted methods of Longuet-Higgins et al [1]. We see this in the single-peak example shown in Figure 1, where both the MLM and IMLM show much better agreement than the LH methods.

Moving to the three-peak example of Figure 2, the (non-iterated) Maximum Likelihood Method shows an ability to resolve the main peaks that is similar to that of the unweighted LH method, while using the Iterated version brings about a closer match to the location and width of the two main peaks. But none of the methods have any ability to resolve the third peak.

3. Comparison of measured and modelled directional spectra

Numerical spectral wave models, such as WAM [10], Wavewatch III [11, 12] and SWAN [13, 14] are now widely used to forecast wave conditions, and in hindcast studies to characterise wave climate. These models all describe the evolution of the directional wave spectrum $S(f,\theta)$. There are limitations in the representation of physical processes and their numerical implementation within these models, and in the inputs forcing them. This makes it essential that simulations are calibrated and verified against available measurements, and records from wave buoys play an important role in this process.

As a first (and most commonly used) level of comparison, integrated statistics such as significant wave height, mean wave period and direction, and directional spread can be used, being quantities that can be readily derived in a consistent way from both model outputs and buoy records. At the next level, more detailed diagnostic information can be obtained by comparing spectra. This is also a robust procedure (in principle) when using the 1-dimensional spectrum $S(f)$, as well as the other "first five" terms which can be directly derived from buoy records, as detailed above.

Ideally, we would like to go to the next level of detail by directly comparing full directional spectra $S(f,\theta)$. from the model with the corresponding quantities from measurements. In, for example, a mixed sea state of multiple swell systems plus local wind sea, such a comparison might highlight that one particular swell component is being poorly represented, leading on to an investigation of errors in the wind fields at the place and time of its initial development.

If, however, we were make such a comparison using a directional spectrum derived from buoy records by one of the methods described above, we need to remember that these derived 2-d spectral estimates are not as robust as the 1-d spectra, otherwise we run the risk of confusing an inaccuracy in the estimated buoy spectrum with an error in the model spectrum.

Hence we seek a method of comparing directional spectra that will use the maximum amount of directional

information obtainable from a buoy record, but no more.

3.1 Method for constructing a diagnostic directional distribution from buoy records using model guidance

Suppose we have a model, using discrete directions $\theta_q,\ q = 1, \ldots Q$ which computes spectral density $S^{(m)}(\theta_q)$. We have dropped the frequency dependence from our notation for convenience, but it should be borne in mind that the following analysis applies at each frequency.

The buoy record gives us a set of five independent cross-spectral estimates $G_p^{(b)}$, for p = 1,...,5. These are just the same terms defined in equations 10-15, re-indexed for convenience.

The "true" spectrum at the same discrete directions that we would like to obtain for comparison with the model is constrained by these cross-spectral estimates, but is otherwise not fully determined by buoy data. Rather, the information available reduces the Q dimensional space of possible values of the discretised directional distribution to a Q-5 dimensional subspace. The buoy record cannot tell us where within this subspace the true directional distribution lies, but we can allow the model estimate to guide us.

We do this by seeking the "diagnostic" directional distribution $S^{(d)}(\theta_q)$ closest to the model's estimate that still satisfies those constraints provided by the buoy cross-spectra

Before we do that, we note that any model involves a degree of error and uncertainty, so we assume that we can attach estimates of the model error $\sigma^{(m)}(\theta_q)$ at some confidence level (say 95%). We can also take into account error estimates $\sigma_p^{(b)}$ for each cross-spectral estimate from the buoy records, at the corresponding confidence level. These are readily estimated alongside the spectral estimates using Welch's averaged periodogram method [15].

Now we can proceed to derive our best fit distribution. We do this by finding the "diagnostic" function $\hat{S}(\theta_q)$ that minimises a quality of fit parameter

$$\chi^2 = \sum_{q=1}^{Q} \Delta\theta \left[\left(\hat{S}(\theta_q) - S^{(m)}(\theta_q)\right)/\sigma^{(m)}(\theta_q)\right]^2 + \sum_{p=1}^{5}\left[(G_p(\hat{S}) - G_p^{(b)})/\sigma^{(b)}(\theta_q)\right]^2 \quad (23)$$

We also have a constraint $\hat{S}(\theta_q) \geq 0$, which makes this a bounded value least squares problem, which can be solved using the algorithm (and Fortran implementation) of Parker and Stark [16].

3.2 Application to parametric test cases

To test this method, we return to the test cases described above, where we assumed the "true" spectrum is a sum of simple parametric distributions (Eqn 22). We also suppose that our "model" produces a similar spectrum, of the same form, with the same number of peaks, but with different central directions, spreading parameters and weightings, to represent the actual errors in the "model". These parameters are listed in Table 1.

For the directional discretisation, Q = 48 bins have been used. We have assumed that all the measured moments have an error $\sigma^{(b)}$ of 2% of their value, while the model errors $\sigma^{(m)}$ are assumed to be of 30%. Note that only the relative value of measurement and model errors plays a role in this method. Here we have deliberately given much higher weighting to the buoy records than to the model.

Table 1. Parameters for the assumed input and "model" directional distributions, as defined in Eqn 22, used in the test cases.

	peak direction	directional spread	weight
	θ_0	$\Delta\theta$ (°)	w
M = 1 test			
input peak 1	60°	20°	0.6
model peak 1	70°	25°	0.55
M = 3 test			
input peak 1	60°	15°	0.45
model peak 1	70°	20°	0.40
input peak 2	150°	30°	0.30
model peak 2	140°	35°	0.35
input peak 3	220°	10°	0.25
model peak 3	230°	15°	0.25

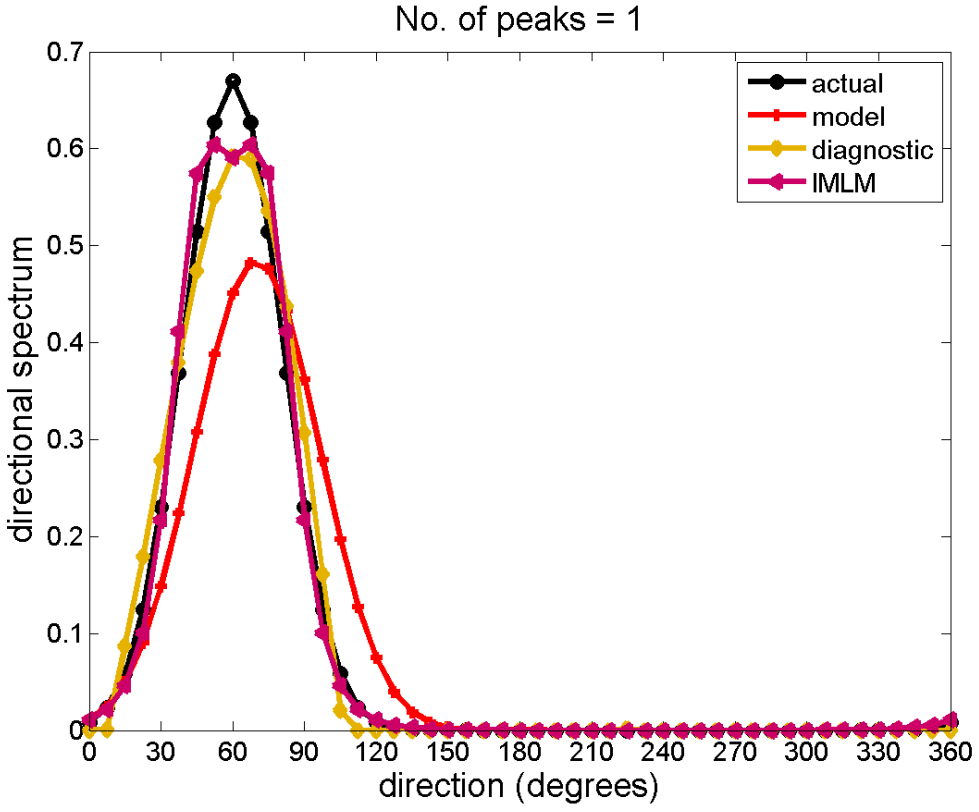

Figure 3 Comparison of a directional distribution of the form $D(\theta) = [\cos(\theta - \theta_0)/2]^p$, with peak direction $\theta_0 = 60°$ and spreading parameter $p = 30$ (black) with the IMLM [5] fit to these data (magenta), a second, independent single-peak "model" distribution (red), and the "diagnostic" distribution obtained by the method described in the present paper (yellow).

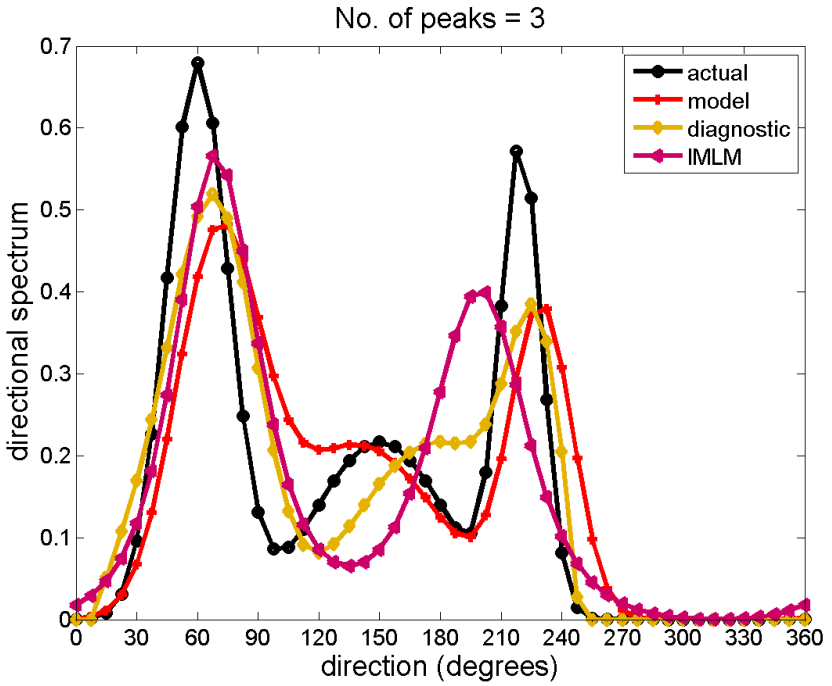

Figure 4 Comparison of a directional distribution combining a weighted sum of three distributions of the form $D(\theta) = [\cos(\theta - \theta_0)/2]^p$ (black) with the IMLM [5] fit to these data (magenta), a second, independent three-peaked "model" distribution (red), and the "diagnostic" distribution obtained by the method described in the present paper (yellow).

The results for the single peak case are shown in Figure 3. This shows a case where we have presupposed that the "model" (red line) has a 10° error in locating the single peak direction, has slightly overestimated the directional spread, and underestimated the total energy.

The "diagnostic" distribution (yellow line) arising from this method gives a very similar result to the IMLM (magenta), relative to which it is only pulled slightly towards the assume "model" distribution.

In the case of the three-peak example (Figure 4), the "diagnostic" distribution is again quite similar to the IMLM result in the vicinity of the largest peak. For the secondary peak, for which we have assumed the model to have captured the width reasonably well, with a moderate offset in peak direction, the "diagnostic" result is more strongly influenced by the "model" distribution. We have also assumed that our "model" does not resolve the third peak very clearly. Consequently, the "diagnostic" solution also struggles to resolve it, but it is encouraging that it shows evidence of its presence at all, something that existing methods are incapable of doing. Further tests not included here indicate that similar results also extend to 4 and 5 peaked distributions.

3.3 Application to Directional Waverider records

We turn now to an application to field measurements, supported by model simulations. The data we consider comes from a Directional Waverider buoy deployed in approximately 76 m water depth off Banks Peninsula, on the east coast of New Zealand's South Island. Figure 5(a) shows the directional wave spectrum computed for 129 discrete frequencies at 0.005 Hz increments from a 30 minute burst sample ending at 21:00 UT on 25/11/2016. The directional distribution over 72 equally spaced directions was estimated using the Iterated Maximum Likelihood Method.

The most prominent feature of the spectrum is a peak at around 0.13 Hz from the NNE (Cartesian direction ~240°), developed from shore parallel winds over much of the previous 24 hours. The local wind at the measurement time had swung to the NW: with a shorter fetch this results in the secondary peak (or possibly a double peak) at higher

frequency. In addition, a SSE swell (0.1 Hz, ~120°) can also be detected, which is typical for this site which has a SE-SW exposure to Southern Ocean sources. We also note small amounts of energy displaced by ~180° in direction from each of the peaks described above.

For comparison, model outputs are available from a wave forecast operated by the National Institute of Water and Atmospheric Research (NIWA). This employed Wavewatch version 3.14 [17] on a New Zealand grid spanning longitudes from 163.21°E to 181.67°E at 15°/512 resolution, and latitudes from 48.54°S to 30.84°S at 10°/512 resolution. This was successively nested in global and regional domains at 15°/64×10°/64 and 15°/128×10°/128 resolutions, respectively. In the spectral domain, 25 frequency bins and 24 directional bins. Atmospheric forcing was provided by the New Zealand Convective Scale Model implementation of the UK MetOffice Unified Model [18].

Figure 5(c) shows the directional spectrum from the model forecast at the nearest grid cell and output time. The forecast spectrum reproduces the general location of the 3 principal sea state components identified in the IMLM estimate from the buoy record (Figure 5(a)). There are differences in the relative contribution of these components, with the forecast giving relatively more weight to the higher-frequency NW wind sea than to the NE component, and being less able to resolve details in the frequency structure. On the other hand, the forecast predicts negligible energy levels where the IMLM estimate gave contributions displaced by 180° from the main peaks.

Figure 5(b) shows the result of applying the procedure described in Section 3.1 above, to produce a merged directional spectrum. The resulting “merged” spectrum retains the directionally-integrated frequency structure from the measured spectrum, hence the relative weighting of the main spectral peaks is not influenced by the model output, only the directional distribution at each frequency. As for the forecast spectrum, the merged spectrum does not show energy at 180° displacement from the main peaks. This illustrates that such components are not a necessary consequence of the “first-5” moments, which are preserved by the merging procedure, but may be a spurious result of the IMLM estimate.

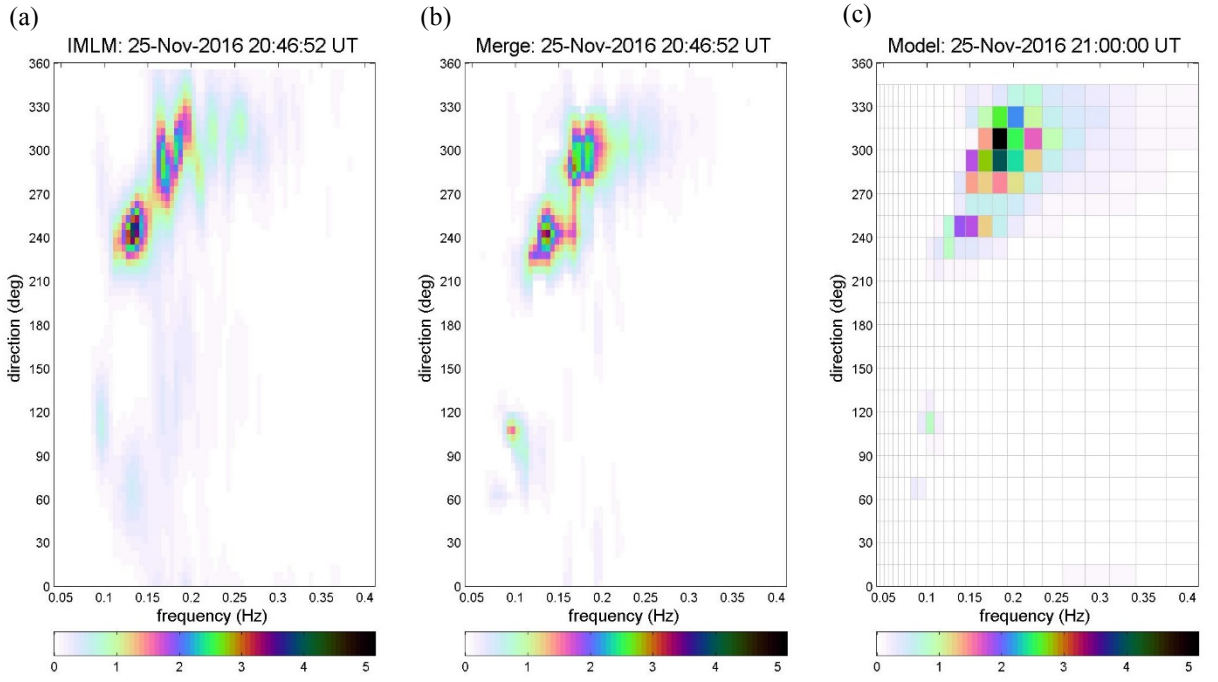

Figure 5 Estimates of the directional wave spectrum from Waverider measurements and a Wavewatch simulation at (42°25´S, 173°20´E), off the east coast of New Zealand’s South Island, at approximately 21:00 UT on 25 November 2016. (a) from

Waverider measurements, using the Iterated Maximum Likelihood Method; (b) derived from a combination of Waverider measurements and model outputs, using the method outlined in this paper; (c) from the Wavewatch simulation. The horizontal axes show wave frequency, while the vertical axes show Cartesian wave direction (i.e. direction towards which waves propagate, in degrees anticlockwise from True East). Colour scales show the estimated spectral density.

4. Discussion

We have presented some initial tests of a method for analysing directional data from wave buoys in a way that can maximise the information that such data can provide for comparisons with directional wave spectra predicted by numerical models. In doing so, we present the concept of a "diagnostic" spectrum, defined as the smallest perturbation of the model spectrum that is fully consistent with the buoy observations.

The point of doing so is not to say that this "diagnostic" spectrum is necessarily a close approximation to the true spectrum, but to use it to identify robust *minimum* values for the errors in the modelled spectrum. This offers potential advantages over comparisons with directional spectra estimated by existing methods, all of which may introduce their own artefacts, especially in mixed sea states of more than two components, for which they inevitably fail.

References

1. Longuet-Higgins, M.S., D.E. Cartwright, and N.D. Smith, *Observations of the directional spectrum of sea waves using the motions of a floating buoy*, in *Ocean wave spectra*. 1963, Englewood Cliffs: New York. p. 111-136.
2. Mitsuyasu, H., et al., *Observations of the directional spectrum of ocean waves using a cloverleaf buoy.* Journal of Physical Oceanography, 1975. **5**: p. 750-760.
3. Isobe, M., K. Kondo, and K. Horikawa. *Extension of MLM for estimating directional wave spectrum*. in *Proc. Symp. on Description and Modeling of Directional Seas*. 1984.
4. Krogstad, H.E., R.L. Gordon, and M.C. Miller, *High-resolution directional wave spectra from horizontally mounted acoustic Doppler current meters.* Journal of Atmospheric and Oceanic Technology, 1988. **5**(2): p. 340-352.
5. Oltman-Shay, J. and R.T. Guza, *A data-adaptive ocean wave directional-spectrum estimator for pitch and roll type measurements.* Journal of Physical Oceanography, 1984. **14**(11): p. 1800-1810.
6. Lygre, A. and H.E. Krogstad, *Maximum entropy estimation of the directional distribution in ocean wave spectra.* Journal of Physical Oceanography, 1986. **16**(12): p. 2052-2060.
7. Hashimoto, N. and K. Kobune. *Estimation of directional spectrum from a Bayesian approach*. in *21st ICCE* 1988. ASCE.
8. Johnson, D., *DIWASP, a directional wave spectra toolbox for MATLAB: User Manual*. 2001, Centre for Water Research, University of Western Australia.
9. Benoît, M., P. Frigaard, and H.A. Schäffer. *Analysing multidirectional wave spectra: a tentative classification of available methods*. in *Proc. IAHR-Seminar: Multidirectional Waves and their Interaction with Structures*. 1997. San Francisco: Canadian Government Publishing.
10. Hasselmann, S., et al., *The WAM Model - a third generation ocean wave prediction model.* Journal of Physical Oceanography, 1988. **18**(12): p. 1775-1810.
11. Tolman, H.L., *A third-generation model for wind waves on slowly varying, unsteady, and inhomogeneous depths and currents.* Journal of Physical Oceanography, 1991. **21**: p. 782-797.
12. Tolman, H.L., *User manual and system documentation of WAVEWATCH-III version 4.18*. 2014, NOAA / NWS / NCEP / OMB. p. 282.
13. Booij, N., R.C. Ris, and L.H. Holthuijsen, *A third-generation wave model for coastal regions 1. Model description and validation.* Journal of Geophysical Research, 1999. **104**(C4): p. 7649-7666.
14. Ris, R.C., L.H. Holthuijsen, and N. Booij, *A third-generation wave model for coastal regions 2. Verification.* Journal of Geophysical Research, 1999. **104**(C4): p. 7667-7681.
15. Oppenheim, A.V. and R.W. Schafer, *Digital Signal Processing*. 1975: Prentice-Hall.
16. Stark, P.B. and R.L. Parker, *Bounded Variable Least Squares: An Algorithm and Applications.* Computational Statistics, 1995. **10**(2).
17. Tolman, H.L., *User manual and system documentation of WAVEWATCH-III version 3.14*. 2009, NOAA / NWS / NCEP / OMB. p. 194.
18. Yang, Y., et al., *Model moist bias in the middle and upper troposphere during DEEPWAVE.* Atmospheric Science Letters, 2017. **18**(4): p. 161-167.